NOTICE CONCERNING COPYRIGHT RESTRICTIONS

This document may contain copyrighted materials. These materials have been made available for use in research, teaching, and private study, but may not be used for any commercial purpose. Users may not otherwise copy, reproduce, retransmit, distribute, publish, commercially exploit or otherwise transfer any material.

The copyright law of the United States (Title 17, United States Code) governs the making of photocopies or other reproductions of copyrighted material.

Under certain conditions specified in the law, libraries and archives are authorized to furnish a photocopy or other reproduction. One of these specific conditions is that the photocopy or reproduction is not to be "used for any purpose other than private study, scholarship, or research." If a user makes a request for, or later uses, a photocopy or reproduction for purposes in excess of "fair use," that user may be liable for copyright infringement.

This institution reserves the right to refuse to accept a copying order if, in its judgment, fulfillment of the order would involve violation of copyright law.

Geothermal Exploration using AVIRIS Remote Sensing Data over Fish Lake Valley, NV

Elizabeth Littlefield and Wendy Calvin

University of Nevada Reno, Reno, NV
eflittlefield@gmail.com • wcalvin@unr.edu

Keywords
Fish Lake Valley, Nevada, remote sensing, AVIRIS, geothermal

ABSTRACT

Fish Lake Valley, in Esmeralda County, Nevada, sits at the southern end of the Mina Deflection where the very active Death Valley-Furnace Creek-Fish Lake Valley fault system makes a right step to transfer slip northward into the Walker Lane. Northern Fish Lake Valley has been pulling part since ca. 6 Ma, primarily along the Emigrant Peak normal fault zone (Stockli et al., 2003). Elevated tectonic activity in Fish Lake Valley suggests there may be increased fracture permeability to facilitate the flow of thermal water. The Fish Lake Valley geothermal prospect is located at the base of the Volcanic Hills, in central northern Fish Lake Valley. Drilling in the region has revealed anomalously high temperatures at depth, but the geothermal system is not yet understood. Geothermal surface expression is limited to localized deposits of siliceous sinter and travertine that occur along a fault.

The Airborne Visible/Infrared Imaging Spectrometer (AVIRIS) instrument acquired hyperspectral data over northern Fish Lake Valley in March 2003. The AVIRIS sensor is maintained by the Jet Propulsion Laboratory and collects data in 224 wavelengths from the visible to shortwave infrared (0.4 to 2.5 μm) at 2 m spatial resolution. The data set covers the Fish Lake Valley prospect and the Silver Peak Range foothills, which are bounded by the Emigrant Peak fault zone. Past studies have successfully used remote sensing data to map hydrothermal alteration as minerals display characteristic spectral signatures. Remote sensing studies compliment traditional field mapping, often identifying alteration minerals that are not obvious in the field. Remote sensing is used to classify mineralogy across very large geographic areas, in this case, ~190 km^2.

The AVIRIS data were processed using statistical and subjective methods to identify hydrothermal alteration minerals including opal, kaolinite, montmorillonite, muscovite, clinochlore, hematite, calcite and borates. Mineral distribution was compared to existing geologic maps, including a surficial geology map by Reheis and Block (2007). We identify previously unmapped deposits of siliceous sinter and several locations with abundant hydrothermal clays that appear to be fault-controlled.

Introduction

Fish Lake Valley Geology

Fish Lake Valley is located within the Great Basin, in Esmeralda County, Nevada. Extensional geothermal systems are common

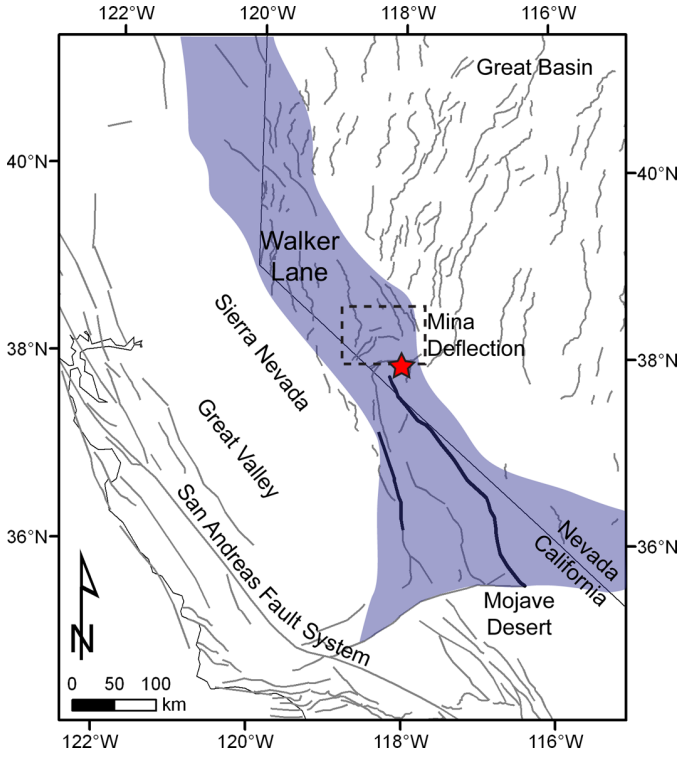

Figure 1. Map of California and Nevada showing the extent of the Walker Lane in blue (modified from Oldow et al., 2001). Bold lines show the Owens Valley and Death Valley-Furnace Creek fault systems. The Owens Valley fault is further west. The dashed outline shows the location of the Mina Deflection and the red star shows the location of Fish Lake Valley.

in the Great Basin because fault fracture-related permeability may allow for deep circulation and heating of meteoric water, and act as a conduit for up-flowing hot water (Wisian et al., 1999). Fish lake Valley is located within the Walker Lane at the southern end of the Mina Deflection, which is a belt of east-trending left-lateral faults (Wetterauer, 1977) (Figure 1). The zone acts as a right step between the right-lateral faults of the Owens Valley and Death Valley-Furnace Creek fault systems, and the right-lateral faults of the central Walker Lane. Northern Fish Lake Valley is one of several pull-apart basins formed as a result of the transfer of right-lateral displacement across the Mina Deflection.

The study area is located in northern Fish Lake Valley, which sits between the White Mountains to the west and the Silver Peak Range to the east (Figure 2.). The northern White Mountains are composed predominantly of granitic plutons, partially overlain by Tertiary volcanic rocks (Albers and Stewart, 1972). The Silver Peak Range is composed of Cambrian and Ordovician metasedimentary rocks, overlain by Tertiary volcanic and sedimentary rocks (Albers and Stewart, 1972). The northwest-trending Fish Lake Valley fault zone (FLVFZ) marks the eastern side of the White Mountains and represents the northern end of the 250 km-long Death Valley-Furnace Creek fault system. The right-lateral FLVFZ is very active with a slip rate of 5 mm/yr since ca. 10 Ma (Reheis and Sawyer, 1997). The fault zone accommodates half the shear transferred from the Pacific-North American plate boundary into the Basin and Range. Fish Lake Valley is bounded to the north by the Coaldale fault, an east-trending fault that is a main structure of the Mina Deflection. The Coaldale fault experienced 60-80 km of movement before the middle Cretaceous and local reactivation during the Cenozoic (Stewart, 1985). The Emigrant Peak fault zone (EPFZ) bounds the valley to the east. This highly active normal fault zone is kinematically linked to the FLVFZ. Elevated slip rates on the local faults likely allow for increased fracture permeability in the adjacent northern Fish Lake Valley.

Bounding Fish Lake Valley to the north are the Volcanic Hills, relatively low lying hills generally composed of Tertiary basalt flows and silicic ash flow tuffs (Figure 2). The Coaldale fault bounds the Volcanic Hills from Columbus Salt Marsh. Reheis et al. (1993) observed a sinter mound, travertine, and siliceous root casts at the base of the Volcanic Hills along a fault. Northern Fish Lake Valley is occupied by a large playa, from which ulexite was mined during the 1870's. Ulexite is a hydrated sodium calcium borate hydroxide, which is significant to this study because borates can be indicative of geothermal systems as they generally form when boron-rich thermal water is evaporated. Coolbaugh et al. (2002) documented a statistical correlation between high boron concentrations and thermal springs in Nevada.

The Fish Lake Valley geothermal prospect is located along the southern part of the Volcanic Hills. The prospect was first discovered in 1970 when a deep oil exploration well drilled by Nevada Oil and Minerals revealed high temperatures (Garside and Schilling, 1979). Since then 13 geothermal wells have been drilled to define the resource (Davis and Hess, 2009), yet the spatial extent is still unknown. Coolbaugh et al. (2006) identified Fish Lake as an area with high geothermal potential, and the U.S. Department of Energy named the valley a "top pick" for geothermal development based on lease type and resource potential (Farhar and Heimiller, 2003).

The Emigrant geothermal prospect is located in the Silver Peak Range foothills, though not within the coverage of the AVIRIS data (Figure 2). This location was identified as a prospect in the 1980's when high temperatures were reported in shallow mineral exploration holes (Hulen et al., 2005). Since then, one deep well has been drilled within the Emigrant prospect, and Hulen et al. (2005) interpret that the geothermal system is related to the en echelon steeply dipping faults that parallel the EPFZ (Figure 2).

Data Collection

Hyperspectral AVIRIS data were collected over Fish Lake Valley on March 19, 2003 (Figure 2). The data were acquired from a DHC-6-200 Twin Otter at an altitude of ~5.05 km above ground level. Data were collected in 224 spectral channels from 0.4 to 2.5 μm and have 2 m spatial resolution.

To increase confidence in mineral maps, some remotely mapped minerals were verified in the field during April 2010. An Analytical Spectral Devices (ASD) FieldSpec Pro portable spectrometer was used in collect spectra from surface materials in the field and from hand samples in the laboratory. The ASD collects high resolution reflectance data in 2,151 spectral channels from 0.35 to 2.5 μm. Mineralogy was identified with reference to the USGS spectral library (Clark et al., 1993).

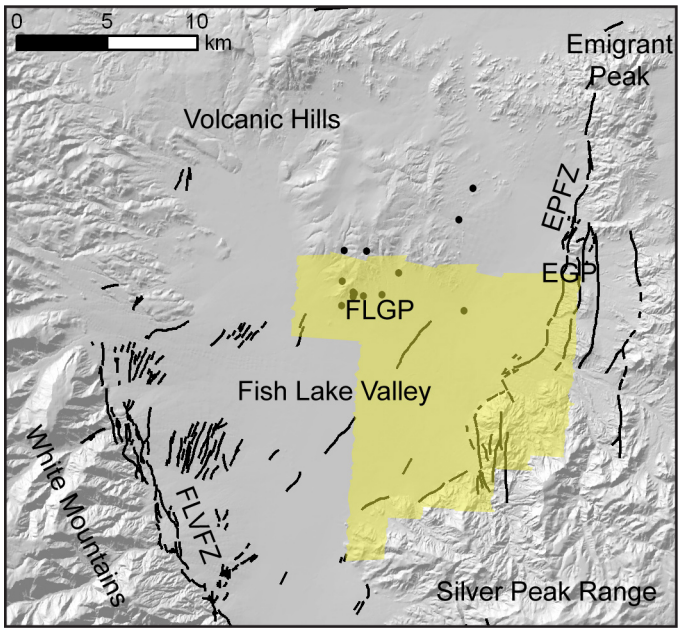

Figure 2. Shaded relief map of northern Fish Lake Valley showing Quaternary faults. The yellow shading shows the coverage of AVIRIS data used for this study, and location of Figure 3. Block dots show the locations of deep geothermal wells. FLVFZ - Fish Lake Valley fault zone, EPFZ - Emigrant Peak fault zone, FLGP – Fish Lake geothermal prospect, EGP – Emigrant geothermal prospect.

Data Analysis

AVIRIS data were supplied as at-sensor radiance and processed using ENVI image processing and data analysis software. The ENVI MODTRAN-based atmospheric correction, Fast Line-of-Sight Atmospheric Analysis of Spectral Hypercubes (FLAASH),

was used to remove atmospheric effects and create surface reflectance images for half the flight lines. The ACORN5B atmospheric correction was applied to the remaining scenes which contained abundant vegetation and required the use of a more flexible algorithm. AVIRIS reflectance data were scaled to surface reflectance measurements using the technique of Clark et al. (2002).

A statistics-based approach was used to identify spectral endmembers from the reflectance data. A Minimum Noise Fraction (MNF) transformation was performed to remove noise from the data. MNF data were subsequently used in a Pixel Purity Index (PPI) calculation to identify spectrally unique pixels. Unique pixels were viewed in ENVI's n-dimensional visualizer tool and spectral classes were identified. The AVIRIS data were also processed using an analyst-biased approach based on techniques that visually highlight spectral differences. A decorrelation stretch (DCS) removes correlation between three input bands to produce a highly saturated color image (Gillespie et al., 1986). Specific minerals were identified by performing DCS of bands surrounding known absorption features. For each scene, a series of DCS images were produced to determine mineral distributions.

Scene endmembers were chosen using both the statistical and DCS approaches to data processing. Spectra from endmember scene pixels were used as input reference spectra for the ENVI Matched Filtering (MF) method. A minimum threshold was applied to MF results to select pixels with spectra similar to the reference spectra. Selected pixels were grouped together in a region of interest (ROI) that could be overlain on any image. Mineralogy was assigned to each ROI based on the comparison of scene spectra to the USGS spectral library. Minerals were displayed using different colored ROIs to create a classification map where each color represents a different surface mineral (Figure 3). Mineral maps were viewed with existing geologic data and National Agriculture Imagery Project (NAIP) photos using ArcGIS software. Especially useful for comparison was a 1:24,000-scale surficial geologic map of Fish Lake Valley by Reheis and Block (2007).

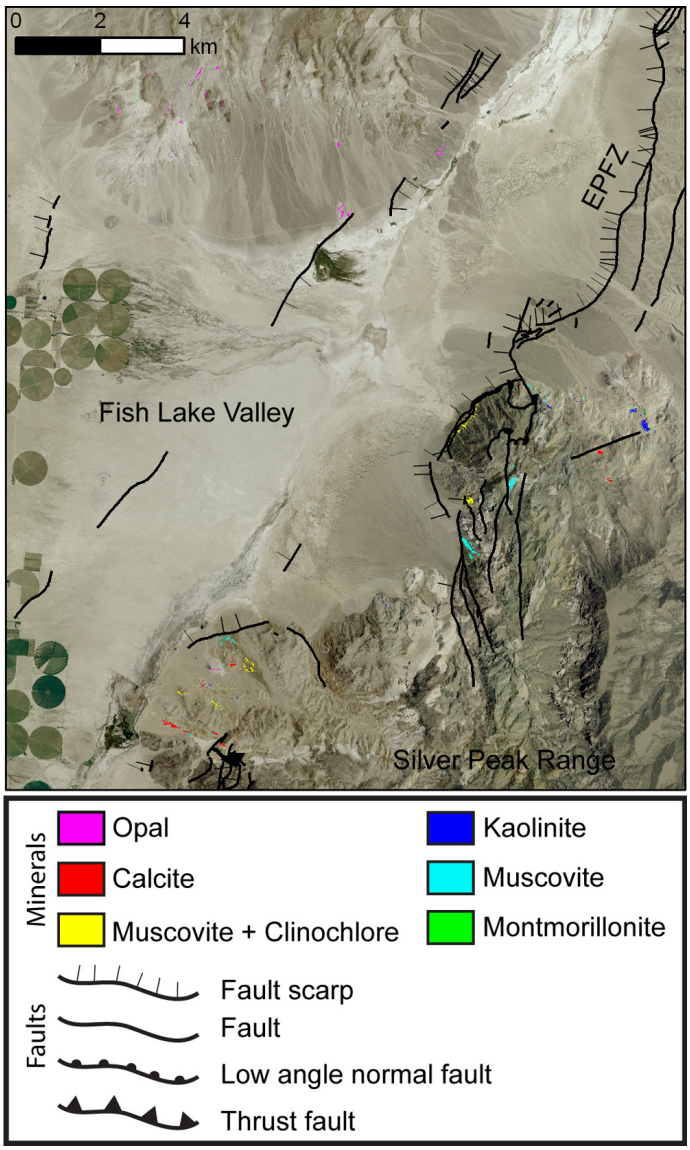

Figure 3. Mineral map derived from AVIRIS data, overlain on NAIP imagery. Faults are from Reheis and Block (2007); inferred, concealed, and certain faults are all shown with the same symbols.

Results and Conclusions

AVIRIS-derived mineral maps were produced to show distribution of geothermal-related minerals in northern Fish Lake Valley (Figure 3). Only minerals mapped with high confidence were included in the maps; confidence was attained when scene spectra clearly matched reference spectra, and upon field validation.

At the southern edge of the Volcanic Hills, kaolinite was remotely mapped adjacent to the drill pad for Fish Lake Power Company's wells 88-11 and 88-11A. This is in the vicinity of the Riek property where there is a tuff-hosted mercury deposit with associated chalcedony, sulfur, gypsum, and cinnabar (Bailey and Phoenix, 1944). The mercury deposit was formed by hot springs at or close to the surface (Bailey and Phoenix, 1944). A field visit verified the remote mapping of kaolinite at this location, and chalcedony, sulfur, cinnabar, and alunite were also observed. Many slickenslides from small faults were observed nearby, and anomalous vegetation indicated there may be water close to the surface. In 1985, commercial temperatures of 204°C and 147°C at 8149 and 8589 ft depths were reported for wells 88-11 and 88-11A, respectively (Davis and Hess, 2009). Plans for a power plant near this location have not come to fruition.

The AVIRIS-derived mineral maps show opal distributed along the southern part of the Volcanic Hills. Field observations validate the presence of opal at eight locations. The AVIRIS data were used to classify both silicified sands and opaline sinter as opal. We remotely identified the large sinter apron discussed by Reheis et al. (1993) and mapped by Reheis and Block (2007), as well as other sinter deposits to the northeast. Reheis et al. (1993) suggested the sinter apron was deposited ca. 0.77 Ma in a hot spring environment near the edge of Pluvial Lake Rennie. Similar rock textures and elevation suggest the sinter at the other locations may also have been deposited along the pluvial lake shoreline. Opal was also mapped along the Emigrant Peak fault on the east side of Fish Lake Valley.

AVIRIS-derived mineral maps also show opal distributed at higher elevations in the Volcanic Hills within Tertiary latite and rhyolite tuffs (Robinson and Crowder, 1973). While the mineral-

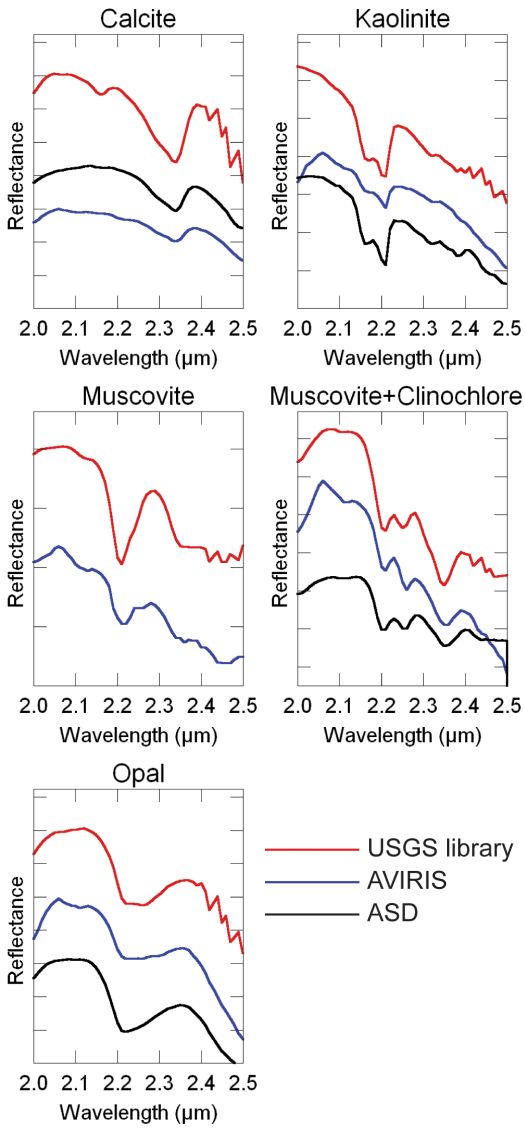

Figure 4. Spectral comparison for some remotely mapped minerals. Red spectra are from the USGS spectral library, blue spectra are from the AVIRIS data, and black spectra were collected from field samples using the ASD spectrometer. USGS and ASD spectra are convolved to AVIRIS wavelengths.

ogy of these deposits has not yet been verified in the field, the reflectance spectra are similar to those of the field-validated opal deposits. Albers and Stewart (1972) mapped many north-trending faults in the Volcanic Hills. These faults may act as conduits for rising thermal waters saturated in silica, resulting in the deposition of opal. Kratt et al. (2009) used ProSpecTIR hyperspectral remote sensing data to map opal/chalcedony in the northern part of the Volcanic Hills.

Calcite was remotely mapped along a fault near the main sinter apron and correlates with travertine mapped by Reheis and Block (2007). Another small outcrop to the northeast was mapped as calcite and is interpreted as travertine. Calcite was also remotely mapped in the Silver Peak Range where it correlates with the Harkless and Poleta Formations mapped by Albers and Stewart (1972); both are Cambrian sedimentary formations that contain limestone units. The calcite mapped in the Silver Peak Range is not related to geothermal activity.

AVIRIS data were used to identify muscovite as well as a combination of muscovite and clinochlore. Muscovite and muscovite/clinochlore distribution correlates with outcrops of the Cambrian Harkless Formation, which is a green phyllitic siltstone (Albers and Stewart, 1972). The formation is composed of silt-sized quartz grains in a matrix of chlorite and muscovite. All rocks of the Harkless Formation are at least slightly metamorphosed (Albers and Stewart, 1972). Clinochlore is attributed to low-grade metamorphism unrelated to recent geothermal activity. Using remote sensing data over Cuprite, Nevada, Rowan et al. (1998) also mapped the Harkless Formation as a muscovite/chlorite mix. Muscovite without chlorite is mapped in the Silver Peak Range, likely where the Harkless Formation is less metamorphosed. The USGS spectral library contains a reference muscovite spectrum from an unaltered sample of Harkless Formation at Cuprite (Clark et al., 2007), which matches the muscovite spectrum from Fish Lake Valley.

Remotely mapped kaolinite, muscovite, and montmorillonite may be products of argillic alteration within the Silver Peak Range. One muscovite deposit is broadly aligned along a fault and may represent alteration by thermal fluids. A second linear distribution of remotely mapped muscovite occurs along another fault, with kaolinite. Abundant kaolinite mapped as a sublinear trend may be related to an unmapped fault. Opal was also mapped in the Silver Peak Range within a small outcrop of Tertiary tuff. These deposits have may be related to geothermal activity; alternatively, kaolinite, muscovite, and montmorillonite may be related to weathering.

Acknowledgements

Funding for this work was provided by the University of Nevada, Reno Vice President for Research Office. AVIRIS data were originally collected through the geothermal programs of LLNL and were provided courtesy of Bill Pickles of the University of California, Santa Cruz.

References

Albers, J.P., and J.H. Stewart, 1972. Geology and mineral deposits of Esmeralda County, Nevada. Nevada Bureau of Mines and Geology Bulletin 78, 80 pp.

Bailey, E.H., and D.A. Phoenix, 1944. Quicksilver deposits in Nevada. University of Nevada Bulletin, v. 38, Geology and Mining Series no. 41, 206 pp.

Clark, R.N., Swayze, G.A., Gallagher, A.J., King, T.V.V., and W.M. Calvin, 1993. The U.S. Geological Survey, Digital Spectral Library: Version 1: 0.2 to 3.0 microns, U.S. Geological Survey Open File Report 93-592, 1340 pp.

Clark, R.N., Swayze, G.A., Livo, K.E., Kokaly, R.F., King, T.V.V., Dalton, J.B., Vance, J.S., Rockwell, B.W., Hoefen, T., and R.R. McDougal, 2002. Surface reflectance calibration of terrestrial imaging spectroscopy data: A tutorial using AVIRIS. Proceedings of the 10th Airborne Earth Science Workshop, JPL Publication 03-4, p. 43-63.

Clark, R.N., Swayze, G.A., Wise, R., Livo, K.E., Hoefen, T.M., Kokaly, R.F., and S.J. Sutley, 2007. USGS Digital Spectral Library splib06a. U.S. Geological Survey, Data Series 231.

Coolbaugh, M.F., Kratt, C., Sladek, C., Zehner, R.E., and L. Shevenell, 2006. Quaternary borate deposits as a geothermal exploration tool in the Great Basin. Geothermal Resources Council Transactions, v. 30, p. 393-398.

Coolbaugh, M.F., Taranik, J.V., Raines, G.L., Shevenell, L.A., Sawatzky, D.L., Minor, T.B., and R. Bedell, 2002. A geothermal GIS for Nevada: defining regional controls and favorable exploration terrains for extensional geothermal systems. Geothermal Resources Council Transactions, v. 26, p. 485-490.

Davis, D.A., and R. Hess, 2009. Nevada Geothermal Well Database List- NV-GEOWEL-2009, February 2020, http://www.nbmg.unr.edu/geothermal/mapfiles.nvgeowel.html, Nevada Bureau of Mines and Geology, Reno, NV.

Farhar, B.C., and D.M. Heimiller, 2003. Opportunities for near-term geothermal development on public lands in the Western United States. DOE/GO-102003-1707, http://www.nrel.gov/docs/fy03osti/33105.pdf, National Renewable Energy Lab., Golden, CO.

Garside, L.J., and J.H. Schilling, 1979. Thermal waters of Nevada. Nevada Bureau of Mines and Geology Bulletin, v. 91, 163 pp.

Gillespie, A.R., Kahle, A.B., and R.E. Walker, 1986. Color enhancement of highly correlated images. I. Decorrelation and HIS contrast stretches. Remote Sensing of Environment, v. 20, p. 209-235.

Hulen, J.B., Nash, G.D., and J. Deymonaz, 2005. Geology of the Emigrant geothermal prospect, Esmeralda County, Nevada. Geothermal Resources Council Transactions, v. 29, p. 369-380.

Kratt, C., Coolbaugh, M., Peppin, B., and C. Sladek, 2009. Identification of a new blind geothermal system with hyperspectral remote sensing and shallow temperature measurements at Columbus Salt Marsh, Esmeralda County, Nevada. Geothermal Resources Transactions, v. 33, p. 481-485.

Oldow, J.S., Aiken C.L.V., Hare, J.L., Ferguson, J.F., and R.F. Hardyman, 2001. Active displacement transfer and differential block motion within the central Walker Lane, western Great Basin. Geology, v. 29, p. 19-22.

Reheis, M.F. and D. Block, 2007. Surficial geologic map and geochronologic database, Fish Lake Valley, Esmeralda County, Nevada, and Mono County, California, scale 1:24,000. Data Series DS-277, U.S. Geological Survey, Denver CO.

Reheis, M.C., and T.L. Sawyer, 1997. Late Cenozoic history and slip rates of the Fish Lake Valley, Emigrant Peak, and Deep Springs fault zones, Nevada and California. Geological Society of America Bulletin, v.109, p. 280-299.

Reheis, M.C., Slate, J.L., Sarana-Wojcicki, A.M., and C.E. Meyer, 1993. A late Pliocene to middle Pleistocene pluvial lake in Fish Lake Valley, Nevada and California. Geological Society of America Bulletin, v. 105, p. 953-967.

Robinson, P.T., and D.F. Crowder, 1973. Geologic map of the Davis Mountain quadrangle, Esmeralda and Mineral Counties, Nevada, and Mono County, California, scale 1: 62,500. Geologic Quadrangle Map GQ-1078, U.S. Geological Survey.

Rowan, L.C., Hook, S.J., Abrams, M.J., and J.C. Mars, 1998. Mapping hydrothermally altered rocks at Cuprite, Nevada, using the Advanced Spaceborne Thermal Emission and Reflection Radiometer (ASTER), a new satellite-imagining system. Economic Geology, v. 98, p. 1019-1027.

Stewart, J.H., 1985. East-trending dextral faults in the western Great Basin: An explanation for anomalous trends of pre-Cenozoic strata and Cenozoic faults. Tectonics, v. 4, p. 547-564.

Stockli, D.F., Dumitru, T.A., McWilliams, M.O., and K.A. Farley, 2003. Cenozoic tectonic evolution of the White Mountains, California and Nevada. Geological Society of America Bulletin, v. 115, p. 788-816.

Wetterauer, R.H., 1977. The Mina deflection—A new interpretation based on the history of the Lower Jurassic Dunlap Formation, western Nevada, Ph.D. thesis, 155 pp., Northwestern University.

Wisian, K.W., Blackwell, D.D., and M. Richards, 1999. Heat flow in the western United States and extensional geothermal systems. Proceedings of the 24th Workshop on Geothermal Reservoir Engineering, p. 219-226, Stanford, CA.